

OPEN ACCESS

Comparing different CFD wind turbine modelling approaches with wind tunnel measurements

To cite this article: Siri Kalvig *et al* 2014 *J. Phys.: Conf. Ser.* **555** 012056

View the [article online](#) for updates and enhancements.

Related content

- [Numerical investigation of the wake interaction between two model wind turbines with span-wise offset](#)
Sasan Sarmast, Hamid Sarlak Chivae, Stefan Ivanell *et al.*
- [The CFD Investigation of Two Non-Aligned Turbines Using Actuator Disk Model and Overset Grids](#)
I O Sert, S C Cakmakcioglu, O Tugluk *et al.*
- [Turbulence characteristics in a free wake of an actuator disk: comparisons between a rotating and a non-rotating actuator disk in uniform inflow](#)
H Olivares-Espinosa, S-P Breton, C Masson *et al.*

Recent citations

- [Large-eddy simulation and experimental study on the turbulent wake flow characteristics of a two-bladed wind turbine](#)
Kun Luo *et al*
- [Simon Gamme *et al*](#)

Comparing different CFD wind turbine modelling approaches with wind tunnel measurements

Siri Kalvig^{1,2}, Eirik Manger³, Bjørn Hjertager¹

¹University of Stavanger, Norway

²StormGeo, Stavanger, Norway

³Acona Flow Technology, Skien, Norway

E-mail: siri.m.kalvig@uis.no

Abstract. The performance of a model wind turbine is simulated with three different CFD methods: actuator disk, actuator line and a fully resolved rotor. The simulations are compared with each other and with measurements from a wind tunnel experiment. The actuator disk is the least accurate and most cost-efficient, and the fully resolved rotor is the most accurate and least cost-efficient. The actuator line method is believed to lie in between the two ends of the scale. The fully resolved rotor produces superior wake velocity results compared to the actuator models. On average it also produces better results for the force predictions, although the actuator line method had a slightly better match for the design tip speed. The open source CFD tool box, OpenFOAM, was used for the actuator disk and actuator line calculations, whereas the market leading commercial CFD code, ANSYS/FLUENT, was used for the fully resolved rotor approach.

1. Introduction

In a cluster of wind turbines, wake effects will result in areas with lower wind velocity than the ambient undisturbed wind, and often higher turbulence levels. Wind farm wake effects will hence result in power losses and increased loading. As there are currently vast investments in offshore wind technology [1], wakes offshore are of particular interest. Due to the lower turbulence regimes that often are present in offshore wind sites, wakes are believed to be more persistent offshore than onshore [2]. Barthelmie et al. [3] showed that wind turbine wakes in large offshore wind farms resulted in average power losses of the order of 10 to 20% of total power output.

Modelling wind turbine performance and wakes is an important but challenging task which can be done using several numerical methods. Sanderse et al. [4] classified the different methods in six groups, with the simplest method, the so-called kinematic method, based on an analytical approach that exploits the far wake to obtain expressions for the velocity deficit and the turbulence intensity. Second in the list is blade element momentum (BEM), followed by vortex methods and panel methods. The final two methods are generalized actuator (which includes the actuator disk, actuator line and actuator surface methods) and what Sanderse calls direct methods. The direct methods include all computational fluid dynamic (CFD) methods that use complete or full modelling of the rotor by the use of body-fitted grids. These two last groups of methods are newer than the first four and quite computationally demanding.



In this paper we perform simulations of a small-scale model wind turbine in a wind tunnel with CFD methods in line with Sande's two last groups, i.e. generalized actuator methods and direct methods. More specifically, the model wind turbine is simulated using the actuator disk method (ADM), the actuator line method (ALM) and a fully resolved method (FRM). The PhD theses of Mikkelsen [5], Réthoré [6] and Troldborg [7] all provide valuable background information on the ADM and the ALM. The FRM has been studied by Zahle et al., [8] amongst others.

Our three different modelling approaches can be organized in terms of accuracy and cost efficiency, with the ADM believed to be the least accurate and most cost-efficient, and the FRM believed to be the most accurate and least cost-efficient. The ALM can be categorized in between the two ends of the scale. The open source CFD tool box OpenFOAM [9] was used for the ADM and the ALM calculations, whereas the market leading commercial CFD code ANSYS/FLUENT [10] was used for the FRM simulations. For all three simulations, Reynolds-averaged Navier-Stokes (RANS) methods were used, but the ALM and FRM simulations are transient and hence unsteady RANS (URANS) was used.

This paper focuses on wake velocity profiles and wind turbine torque and thrust. Results from the ADM, ALM and FRM are compared with each other, as well as with experimental results. The motivation for this is to gain knowledge on the different CFD methods available for wind turbine performance simulations and to provide recommendations for further usage.

2. Wind tunnel experiment and general simulation characteristics

In October 2011, the authors participated in blind test predictions of a model wind turbine organized by Nowitech¹ and Norcowe² in Bergen, Norway. Eight independent modelling groups submitted 11 sets of simulations, and the results from the blind test calculations are presented by Krogstad et al. [11]. In this current paper, the blind test contributions of Kalvig (ADM) and Manger (FRM) are further described and analyzed, and we have performed additional simulations and included the ALM in the comparison.

The length of the wind tunnel is 11.15 metres. The wind tunnel height increases slightly downstream. The height at the inlet is 1.80 metres and at the outlet 1.85 metres. This increasing tunnel height will limit the effect of the walls when the wake expands.

The turbine was located 3.66 m away from the inlet. The model wind turbine, with the National Renewable Energy Laboratory (NREL) s826 airfoil, had a rotor diameter of 0.89 m, and the centre of the rotor was located 0.82 m above the wind tunnel floor (see Figure 1). The rotor speed for the design tip speed ratio was 1282 rpm, giving a rotor tip Reynolds number of 103600. A grid at the tunnel inlet is used to create a turbulent field.

Both thrust and torque, as well as wake velocity, were measured in the wind tunnel. The velocity was measured using a hot-wire anemometer with an x-probe. The sampling rate was 14 kHz in 60 seconds. More information about the experiment can be found in [12, 13].

The ADM and FRM were performed as a part of the blind test in October 2011, but the ALM simulations were done later. In this study we have left the "blind-test principle". In order to run the ALM code, several input parameters need to be determined and in this process one of the input parameters has been tuned to the known turbine power output.

All three methods use the same boundary conditions. The given inlet condition for the blind test experiment was uniform inflow with a reference wind speed of 10.0 m/s and a turbulence intensity of 0.3%. These were used as boundary conditions at the inlet. The inlet boundary condition for dissipation was calculated based on the information given about the hydraulic diameter of 2.19 m. No slip conditions were used for the walls. The outlet boundary condition was zero gradient. All three methods use a two-equation turbulent closure. ADM and ALM use the standard k- ϵ model [14] and the FRM uses the SST k- ω model [15]. ADM is steady state, and ADL and FRM are transient simulations. Further simulation details are summarized below.

¹ Norwegian Research Center for Offshore Wind Technology, <http://www.sintef.no/projectweb/nowitech/>

² Norwegian Centre for Offshore Wind Energy, <http://www.norcowe.no/>

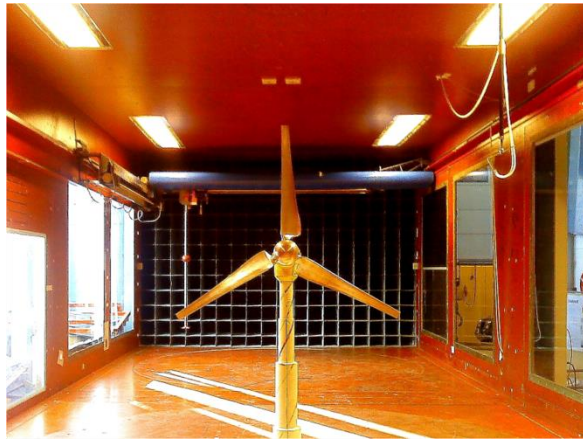


Figure 1: The model wind turbine in the wind tunnel, NTNU.

3. Actuator disk simulations

The actuator disk method (ADM) is based on momentum theory – the model turbine rotor is represented by a “disk” extracting momentum from the flow. Disk area (D), power coefficient (C_P) and thrust coefficient (C_T) are all input values to the model. Values for C_P and C_T were obtained from a performance test which Krogstad et al. [15] carried out in 2010. Here, C_P and C_T were measured for the model wind turbine. The simulations were performed for tip speed ratios (λ) 3, 6 and 10, with OpenFOAM using a steady state solver for incompressible, turbulent flow. Turbulence was modelled utilizing the standard $k-\epsilon$ model [14].

OpenFOAM is an open source computational toolbox containing various applications and utilities for finite volume simulations. A main advantage of OpenFOAM is that the program is open and free of charge, with a flexible structure, allowing the user to access and modify the code. Parallel runs on multiple processors can be performed without additional license costs. In OpenFOAM version 1.7.0, released in June 2010, the solver “simpleWindFoam” was distributed by the OpenFOAM Foundation [17]. This solver and setup formed the basis for the actuator disk simulations. The OpenFOAM tool “snappyHexMesh” was used to create the grid. The grid was refined in a region near the disk, see Figure 2, but not near the walls. The turbine tower was not modelled. Grid dependency tests were performed, and the solution is believed to be grid independent for velocity calculations. The final grid size used was 1.7 million cells, and the results presented are from 500 iterations; then the convergence criterion of 10^{-4} was reached.

4. Actuator line simulations

As for the ADM, the actuator line method (ALM) also relies on an actuator device extracting momentum from the flow. However, instead of having a disk with uniform distributed force, the rotor blades are now represented as span wise sections with airfoil characteristics. In the actuator line methodology of Sørensen and Shen [18], blade loading is implemented in these span wise sections and introduced in the Navier-Stokes equations as a body force. Churchfield [19] implemented the ALM of Sørensen and Shen in the toolbox OpenFOAM, and this is the basis for our ALM simulations. We have used the setup with the transient solver “pisoFoamTurbine”. This was originally intended for large eddy simulations (LES), but we have changed the setup to use unsteady RANS (URANS).

The method requires airfoil look-up tables, i.e. an airfoil file containing a list of lift and drag coefficients versus angle of attack. The freeware airfoil development system XFOIL [20] was used to generate the required airfoil data, and the S826 airfoil geometry was found in the article by Somers

[21]. The airfoil data used here was created by John Amund Lund at Meventus³, and a closer description of the XFOIL generated airfoil data can be found in [22]. The local blade Reynolds number, calculated on the basis of rotational speed and representative chord length, will vary along the blade, and in [22] a wide range of XFOIL calculations were made in order to account for Reynolds number sensitivity. These simulations were made by considering the blade as different airfoils, with the one closest to the rotor being simply a cylinder, and drag/lift coefficients for the four others being determined on the basis of different Reynolds numbers, in the range of 10000-150000. The simulations were performed for tip speed ratios (λ) 3, 6 and 10.

Unlike the ADM, ALM allows us to study wind turbine forces and information along the blade radius. Thus, thrust and torque are calculated for the model wind turbine. Several input parameters needed to be established in order to perform the ALM simulations and these are summarized in 4.1.

The grid was generated with the OpenFOAM tool “blockMesh”. It is refined in a region around the rotor, but not near the walls. The method does not include the turbine tower and this is not modelled. Grid independency tests were performed, and the solution is believed to be grid independent for velocity calculations. The final grid size used was 2.4 million cells.

While Fredriksen [23] worked with the ALM code during his master thesis, the code was changed from explicit scheme to implicit scheme, and we have used this modification to the original code as well in the result presented here. By including the calculation of the wind turbine forces within the PISO algorithm [24], a tighter coupling between the flow field and the turbine blades was ensured. This change also made the code more robust regarding the time step size.

Martínez et al. [25] recommended that the time increments should be small enough so that the tip only passes through one local grid cell during each time step. For all simulations the time increment has been $2.5 \cdot 10^{-4}$ seconds, and this ensures that the blade tip will not pass through more than one local grid cell for the different simulations that were used in the grid independency test (from 350 thousand to 4 million cells) as well as the final simulations that are used later in this study.

The simulation time was 5 seconds. Since the rotor speed is very high for this small model wind turbine, this simulation time is believed to be enough in order to establish a quasi-steady result.

4.1. *Input parameters in the actuator line method*

ALM relies on various input values. Among others, the Gaussian width parameter and the number of the actuator line elements need to be chosen. It is also possible to use a correction term in order to allow the lift to approach zero more gradually at the tip and root of the blade. Martínez et al. [25] found that using Glauert tip- and root-loss correction terms decreased the predicted power. The result presented here is with the tip- and root-loss correction term (Table 1).

An important input parameter in the OpenFOAM setup by Churchfield [19] is the Gaussian width parameter that controls how the forces are distributed along the lines representing the rotors. Some publications exist regarding how to establish a representative Gaussian width parameter. Trolldborg [7] recommends that the parameter should be larger than twice the local grid cell length. In Martínez et al.’s [25] experience, this was also good guidance in order to avoid numerical instabilities in the solver. The latest work of Churchfield [26] states, however, that the Gaussian width parameter should also correspond to a representative blade chord length. The master thesis of Nodeland in 2013 [27] also reaches the same conclusion after extensive testing of the ALM. It is still difficult to establish a physically appropriate value of the Gaussian width parameter, and this is ongoing research.

Based on the guidance [26], we have performed the following procedure to establish an appropriate Gaussian width parameter for the simulations presented here: grid independency tests were performed. Thereafter we ran three simulations with different Gaussian width parameters. A cubic spline interpolation was used to fit the Gaussian width parameter to the known power of 172 W. Then a Gaussian width parameter of 0.0214 was used as input to the new simulations presented here.

³ Meventus is a Norwegian and Denmark based wind energy company, www.meventus.com

The ALM also requires an input parameter that states the number of actuator line elements, into which one blade should be divided. [25] recommended that for each grid cell across the blade, there should be at least 1.5 actuator line elements. In the following we have chosen the actuator line elements to be 46, which is twice the number of grid cells across one blade, in line with the suggestion in [27].

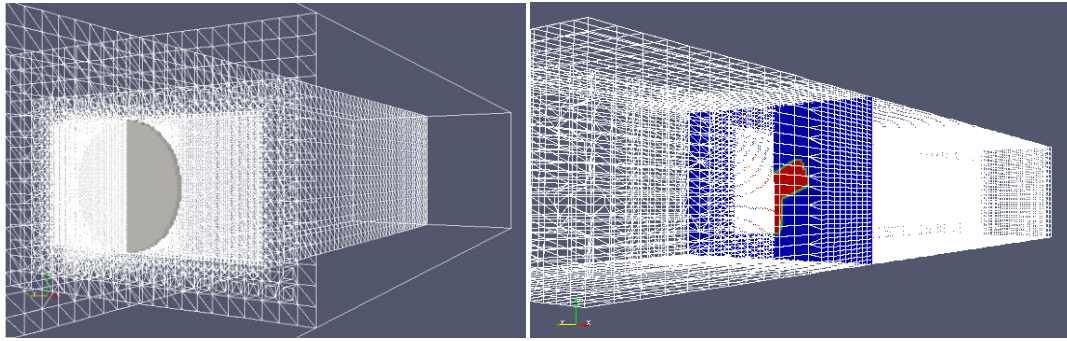


Figure 2: Wind tunnel domain, 11.15 m, 2.71 m and 1.851 m. Left: Actuator disk domain, the actuator disk is located 3.66 m downstream of the inlet and visualized as a 0.04 m thick disk. Right: Actuator line domain, body force is visualized on a slice.

5. Fully resolved rotor method

The fully resolved rotor (FRM) calculations were performed using ANSYS/FLUENT. In these calculations, the exact layout of the wind turbine is modelled geometrically and simulated using a sliding mesh technique. The method requires a fine resolution near the blade to obtain accurate predictions, which again means many computational cells. The mesh used here has approximately 5.3 million cells. In addition, the calculations must be performed using a transient solver, since the actual motion of the rotor is modelled directly during the simulations. Therefore, substantial computer resources are required to perform these calculations.

Figure 3 shows parts of the mesh used in the simulations, focusing around the turbine rotor. The blades of the turbine are meshed using squares and a mapped face mesh, ensuring the best possible mesh quality in this region. The left part of the figure shows the boundary layer, which is resolved down to $y^+ \sim 5$ for best possible accuracy.

Accurate results are highly dependent on the capability of predicting separation and re-attachment on the blade correctly – a few percent off here can give large deviations from measurements. The $k-\epsilon$ model, as used for the ADM and the ALM, is known to have poor properties with respect to correct prediction of recirculation, separation and re-attachment. The SST $k-\omega$ model by Menter [28] has, however, proved to predict flow around airfoils quite accurately. The model is a blend between the standard $k-\omega$ model near the wall and a transformed $k-\omega$ model in the free stream. The SST $k-\omega$ model is thus selected as turbulence model for the FRM calculations.

Typical time steps for the FRM model were around 10^{-3} seconds, somewhat depending on the tip speed ratios. The simulations were run until a quasi-steady state solution was achieved, typically some 2-3 seconds, before obtaining averaged quantities that are reported here.

To save computational time, the transient simulations are started from a solution computed with a moving reference frame (MRF) model. In this approach, the motion sources from the rotating parts are accounted for, but the mesh itself is static. This allows steady state simulations, and an average velocity field can be found and used as a starting point for the more accurate transient calculations.

Compared with the actuator disk and the actuator line modelling approaches, the fully resolved rotor simulations do not require any input constants; drag and lift are calculated directly by the code, as well as the velocity patterns in the wake.

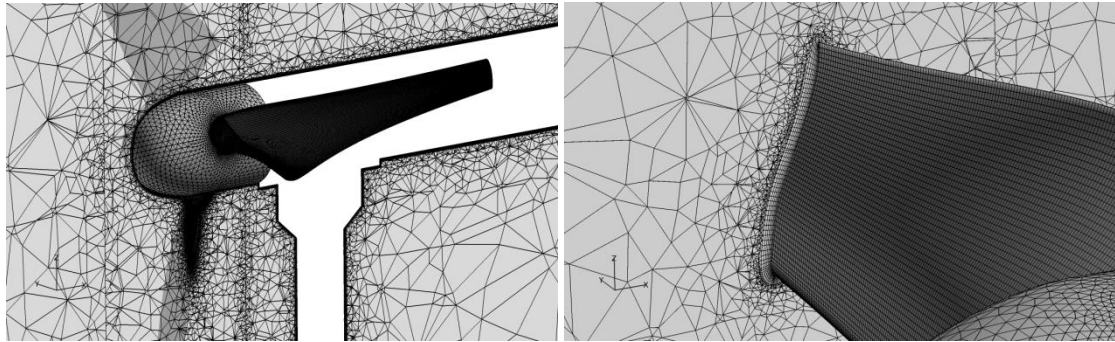


Figure 3: Details of the mesh around the turbine and its blade. The left part of the figure shows the boundary layer created around the blade profile.

6. Results

The wake velocity profiles' results from the different methods are presented first and compared with measurements and then compared with each other. Only the results from the design tip speed are used in the presentation of the wake velocity. Thereafter wind turbine forces are compared between ALM and the FRM for three different tip speeds.

6.1. Actuator disk wake velocity profiles

The ADM simulations of the velocity profiles exhibit the characteristic “top hat” shapes; see Figure 4. Since the rotor is represented as a disk with uniform momentum extraction, the variation in the wake velocity from tip to rotor is not captured. The velocity levels in the far wake⁴ ($X/D=5$) are best captured. The asymmetry in the measurement is believed to be a result of the interaction between the rotor blades and the tower. The tower would normally produce a lower velocity in the shadow with corresponding velocity increase in its vicinity. The turbine blades, however, set up a rotation so that the tower shadow is skewed with a larger velocity increase on one side of the tower. In the ADM simulations the tower is not modelled, and this asymmetry is thus not captured. Close to the tip of the rotor, the wind speeds up and exceeds the reference velocity. This speed-up is less than the measurements. These results indicate that the ADM can to some extent predict the far wakes by the use of a steady state simulation, and this can be a very attractive and computationally effective approach for wake studies in wind farms.

⁴ The wake region is divided into near and far wake, with the near wake being the region just behind the rotor to approximately one rotor diameter downwind and the far wake being the area after the near wake [21].

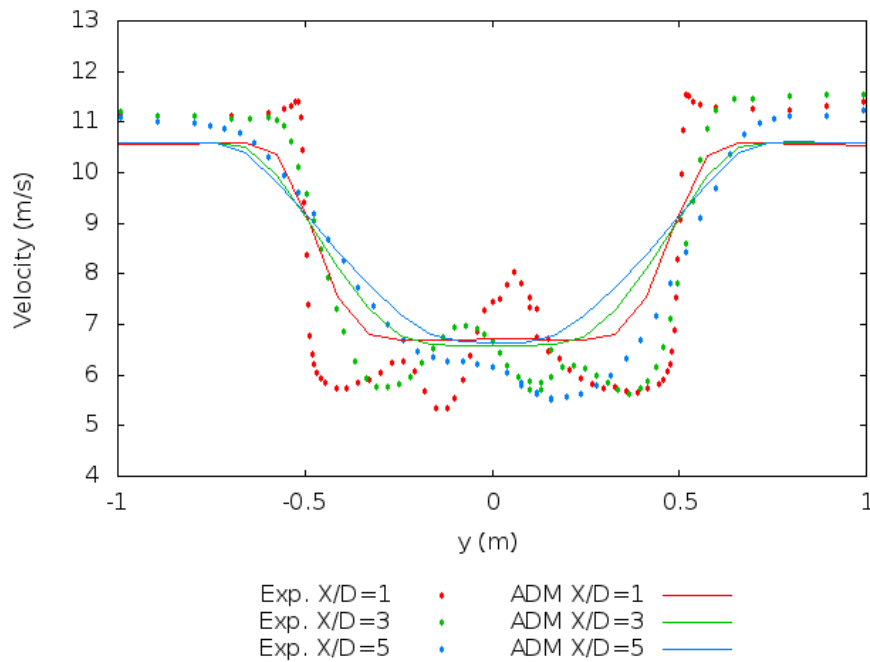


Figure 4: Horizontal wake velocity profiles simulated with ADM (design tip speed) and compared with measurements (Exp.) for different positions downwind, $x/D=1$, $x/D=3$ and $x/D=5$, where D is the diameter of the rotor.

6.2. Actuator line wake velocity profiles

The ALM calculations capture the relative variation of the velocity levels in the wake, but as seen in Figure 5, the velocity at the hub is seriously over estimated. The nacelle is not modelled, and too much wind passes by the centre of the nacelle. The tip velocity wake is best captured for the near wake, i.e. at $X/D=1$. Also the wake in the region outside the rotor is best captured for the near wake.

The Gaussian width parameter used here corresponds to 1.0899 of the local grid cell of 0.0196 m. This is in contrast to [7] and [25], which recommended that the lower limit for the Gaussian width parameter should be no smaller than twice the local grid cell length. They experienced numerically unstable solutions for too small Gaussian width parameters. We did not experience numerical instability, even though our Gaussian width parameter values were less than this limit. The fact that we have changed the code from explicit scheme to implicit scheme can imply that the codes are not comparable. Also, while the previous work was based on LES, we used URANS and this could also be part of the reason for this inconsistency in the Gaussian width parameter settings.

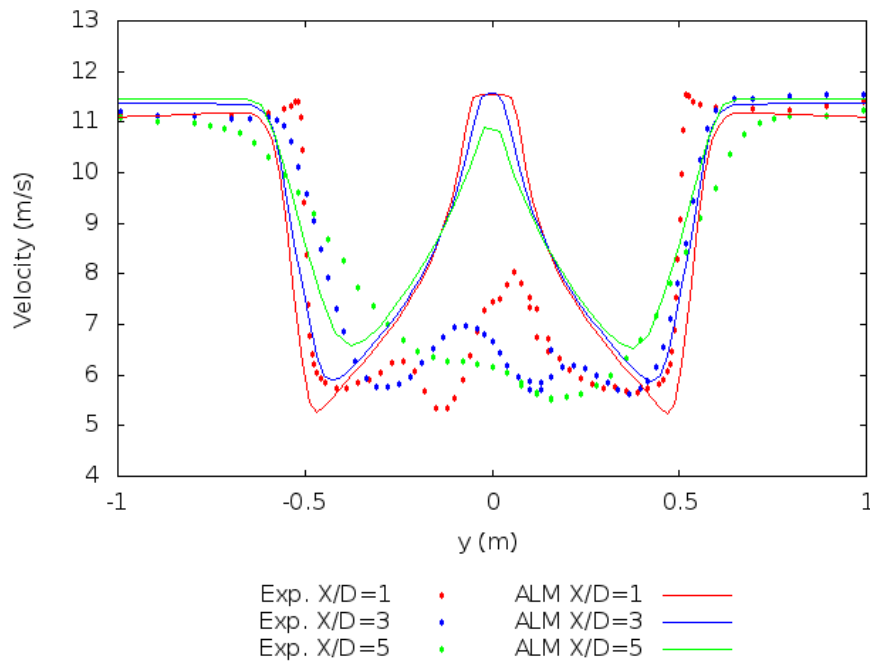


Figure 5: Horizontal wake velocity profiles simulated with ALM (design tip speed) and compared with measurements (Exp.) for different positions downwind, $x/D=1$, $x/D=3$ and $x/D=5$, where D is the diameter of the rotor.

6.3. Fully resolved rotor wake velocity profiles

The FRM simulation captures well the variation in the wake. The agreement with experiments is good for all positions, but best for the near wake, as seen in Figure 6. Part of the reason for the increasing deviation with increasing distance is believed to be too short calculation time and thereby insufficient averaging. As stated earlier, the FRM calculations are time-consuming, and the lack of available computer resources limited the simulation time. Note the asymmetry, present both in the experiments and in the simulations. This feature, also quite well captured in the predictions, is caused by the interaction between the turbine tower and the rotor blades, commented on earlier. Velocity contours behind the wind turbine are visualised in Figure 7.

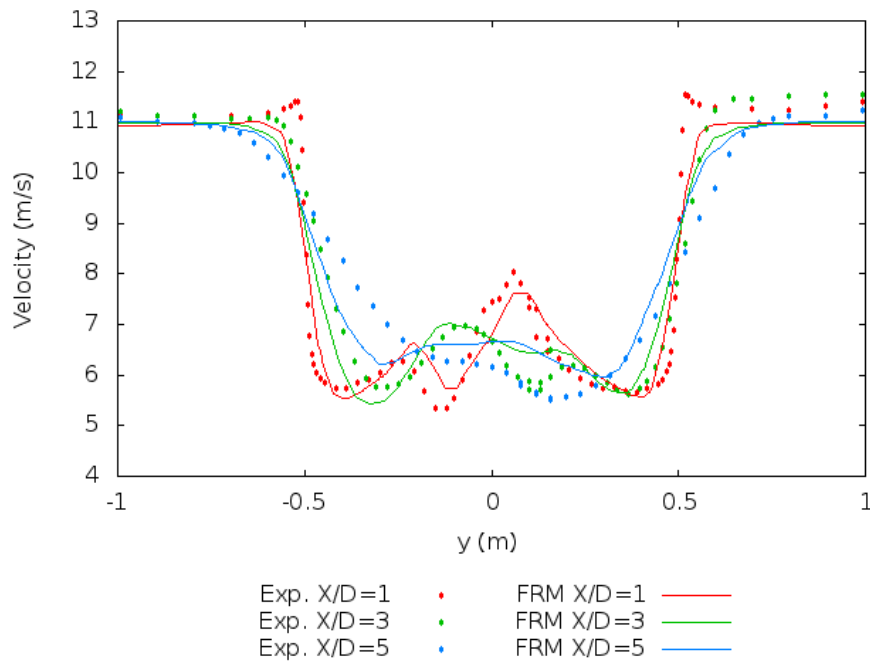


Figure 6: Left: Horizontal wake velocity profiles simulated using FRM (design tip speed) and compared with measurements (Exp.) for different positions downwind, $x/D=1$, $x/D=3$ and $x/D=5$, where D is the diameter of the rotor.

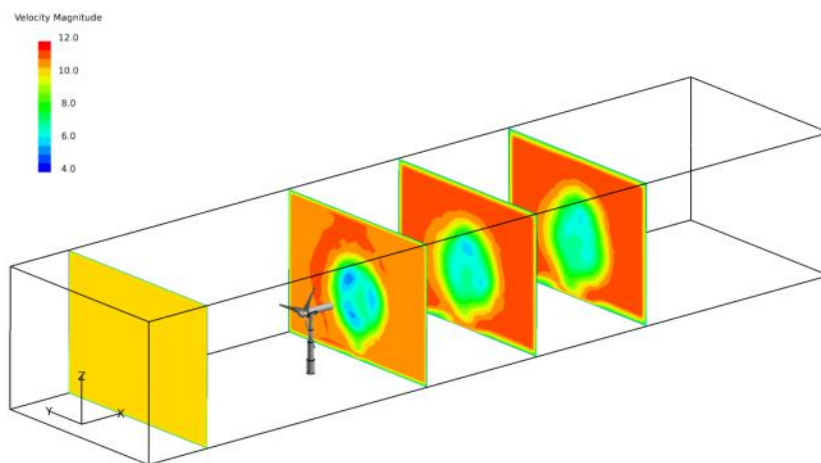


Figure 7: In the fully resolved rotor method, the whole wind turbine with the tower was modelled. Here predicted velocity pattern behind the wind turbine is displayed for position $x/D=1$, $x/D=3$ and $x/D=5$. Blue indicates areas with low wind, whereas the red areas indicate higher wind.

6.4. Simulations compared with each other

In Figure 8 simulations' results from near wake ($X/D=1$) and far wake ($X/D=5$) are compared with each other and with experiment values. The FRM stands out as the most accurate model and produces wake velocity values that are close to the experiment values, especially for the near wake. The ADM results for the far wake fit better to the experimental values than those for the near wake. The ALM results, on the other hand, show larger deviation for the far wake than for the near wake.

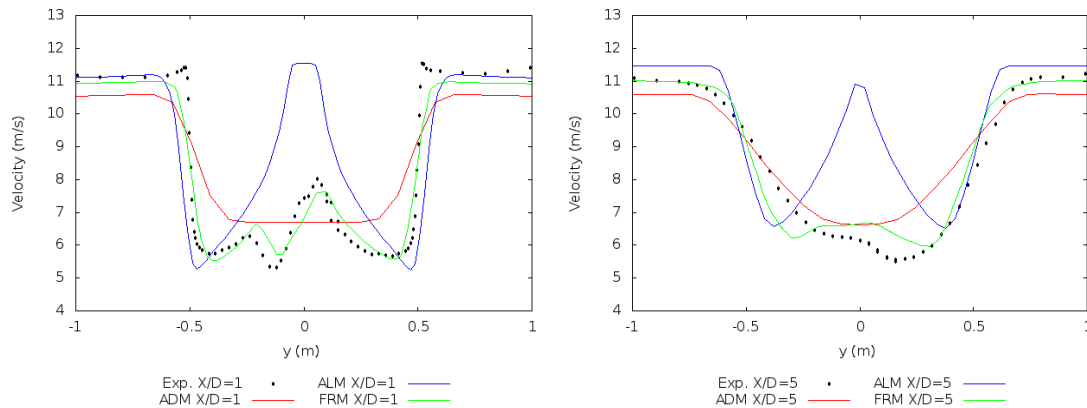


Figure 8: ADM, ALM and FRM compared with each other and with measurements for one and five rotor diameter downwind for tip speed ratio 6.

6.5. Wind turbine forces' calculations from ALM and FRM

This version of ADM does not give information about wind turbine forces, and only results from ALM and FRM can be compared against the experimental data. Table 1 lists the experimental values of C_P and C_T , and the measured values are compared with the estimated values from the two different simulation approaches.

As expected the design tip speed is easiest to model, and the simulated power and thrust compare best with the experiment values for the design speed. The FRM predicts values close to the experimental values, slightly overestimating C_P by 2% and underestimating C_T by 8%. The simulation performed with ALM gives practically the same values for C_P as in the experiment and approximately 7% underestimation on the thrust.

For tip speed ratios 10 and 3, both the FRM and ALM results are far off. The largest deviations from the experiment values for FRM are for tip speed 3 and for ALM are for tip speed 10.

Tip speed ratios		Experiment	FRM	Deviation	ALM	Deviation
3	C_P	0.12	0.23	91.6 %	0.17	43.3 %
	C_T	0.40	0.46	15.0 %	0.34	- 15.3 %
6	C_P	0.45	0.46	2.2 %	0.45	0.8 %
	C_T	0.92	0.85	- 7.6 %	0.86	- 6.7 %
10	C_P	0.20	0.16	- 20.0 %	0.04	- 80.1 %
	C_T	1.17	1.03	- 12.0 %	0.88	- 24.4 %

Table 1: Power coefficient (C_P) and thrust coefficient (C_T) from FRM and ALM simulations for different tip speed ratios (λ) are compared with experimental values.

7. Discussion and conclusions

Wake velocity profiles, torque and thrust are fairly well predicted using a fully resolved rotor approach for the design tip speed ratio 6. For the wake simulations there are, however, larger discrepancies in the results from the ADM and the ALM approaches. Both the FRM and the ALM predicted power and thrust are very close to the measured values for the design tip speed; for the other tip speed ratios, the deviations were somewhat larger.

The ADM performs best on far wakes, where the magnitudes of the wake velocity deficit are in line with measurements. It would be interesting to study the performance of this model for positions further downwind, as the results are promising for far-wake predictions. The actuator disk method does not capture any variation over the rotor blade since the method used is a simple uniform actuator disk model.

The ALM, on the other hand, captures the variation pattern, but it is far off in magnitude for both near and far wake for the hub area. For a realistic turbine, the nacelle is believed to be of relatively less importance than for this down-scaled version of an operational wind turbine.

Réthoré et al. [6] report that the standard k - ϵ model is known to under-predict the wake effects and suggest LES instead. This could be an explanation, but in order to investigate this, we need to perform the same simulations with LES and compare the results. In this study we have focused on wake velocity and turbine forces, but turbulence characteristics in the wake are of course also of great interest. In order to compare turbulence levels between these three different methods, more work and investigations have to be carried out. Churchfield et al. simulated wake losses for Lillgrund wind farm [26], and the simulated time-averaged power production of the wind farm agrees well with Lillgrund field observations. There is reason to believe that the large discrepancies in the wake prediction for this small-scale model wind turbine are greater than would be the case for a full-scale wind turbine. Both the high rotational speed of the small-scale turbine and the relative large size of the nacelle (that the ALM does not model) complicate the calculations compared to a large scale wind turbine. Detailed field measurement in the wind turbine wake is sparse, and further study of the ALM must be performed in order to conclude on this matter.

The ALM is dependent on correct input values and setup. The method is also found to be quite sensitive for the composition of the airfoil data. The Gaussian width parameter has, in particular, a great influence on both the wake velocity predictions and the calculation of the wind turbine forces. Currently there is no uniform way of establishing appropriate Gaussian width parameters without model tuning. Nevertheless, the ALM results are promising for wind turbine force investigations, especially for the design tip speed.

In this study the FRM produces superior wake velocity results compared to the ADM and ALM and on average it also produces better results for the force predictions, although the ALM had a slightly better match for the design tip speed.

The good results, close to the measured values for both wake velocity profiles and forces' calculations with the FRM simulation, suggest that this setup can be further utilized in model tuning and in an examination of both the ADM and the ALM approaches. Measurements from both real wind farms and wind tunnels are sparse and often costly, whereas the FRM setup, on the other hand, can easily be modified and hopefully serve as a way to benchmark the other models.

Acknowledgements

We would like to acknowledge Mr John Amund Lund at Meventus for the use of his xFOIL generated airfoil data.

This work was made possible by funding from the Norwegian Research Council Industrial PhD-program (198257) and from StormGeo. The work is also a part of the Norwegian Centre for Offshore Wind Energy (NORCOWE) under grant 193821/S60 from the Research Council of Norway (RCN). NORCOWE is a consortium with partners from industry and science, hosted by Christian Michelsen Research.

References

- [1] European Commission 2009 Press release: Commission welcomes adoption of climate and energy. Brussels, 23 April 2009
- [2] Barthelmie R, Larsen G, Pryor S, Jørgensen H, Bergström H, Schlez W, Rados K, Lange B, Vølund P, Neckelmann S, Mogensen S, Schepers G, Hegberg T, Folkerts L and Magnusson M 2004 ENDOW (efficient development of offshore wind farms): modelling wake and boundary layer interactions. *Wind Energy* **7** (3): 225-245
- [3] Barthelmie RJ, Hansen K, Frandsen ST, Rathmann O, Schepers JG, Schlez W, Phillips J, Rados

- K, Zervos A, Politis ES and Chaviaropoulos PK 2009 Modelling and measuring flow and wind turbine wakes in large wind farms offshore. *Wind Energy* **12**: 431-444 doi: 10.1002/we.348
- [4] Sanderse B, van der Pijl SP and Koren B 2011 Review of computational fluid dynamics for wind turbine wake aerodynamics. *Wind Energy* **14**: 799-819 doi: 10.1002/we.458
- [5] Mikkelsen R 2003 Actuator disc methods applied to wind turbines. PhD Thesis, Department of Mechanical Engineering Technical University of Denmark, June 2003
- [6] Réthoré P-E 2009 Wind turbine wake in atmospheric turbulence. PhD Thesis, Ålborg University, October 2009
- [7] Troldborg N 2008 Actuator line modeling of wind turbine wakes. PhD Thesis, Technical University of Denmark, Lyngby, Denmark
- [8] Zahle F and Sørensen NN 2007 On the influence of far-wake resolution on wind turbine flow simulations. *J. Phys.: Conf Series* **75** 012042
- [9] OpenFOAM <http://www.openfoam.com/> accessed September 2012
- [10] ANSYS/FLUENT <http://www.ansys.com/> accessed September 2012
- [11] Krogstad PÅ and Eriksen PE 2013 ‘Blind test’ calculations of the performance and wake development for a model wind turbine. *Renew. Energ.* **50** 325-333 ISSN 0960-1481, 10.1016/j.renene.2012.06.044
- [12] Krogstad PÅ, Eriksen P and Melheim J 2011 ‘Blind test’ workshop. Department of Energy and Process Engineering, NTNU, 30 March 2011
- [13] Krogstad PÅ and Eriksen PE 2013 ‘Blind test’ calculations of the performance and wake development for a model wind turbine. *Renew. Energ.* **50** February 2013, 325-333, ISSN 0960-1481, <http://dx.doi.org/10.1016/j.renene.2012.06.044>
- [14] Launder BE and Spalding DB 1974 The numerical computation of turbulent flows. *Comput. Meth. Appl. M.* **3** March 1974, 269–289
- [15] Menter FR, Kuntz M and Langtry R 2003 Ten years of experience with the SST turbulence model *Turbulence, Heat and Mass Transfer* **4** 625-632 (Begell House Inc.)
- [16] Krogstad PÅ, Karlsen J and Adaramola M 2010 Performance of a model wind turbine *17th Australian Fluid Mechanics Conf.* New Zealand
- [17] OpenFOAM Foundation release June 2010 <http://www.openfoam.org/download/version1.7.0.php> accessed August 2012
- [18] Sørensen JN and Shen WZ 2002 Numerical modeling of wind turbine wakes. *J. Fluid Eng.* **124** 393-399 DOI: 10.1115/1.1471361
- [19] Churchfield MJ, Lee S and Moriarty P 2012 Overview of the simulator for offshore wind farm application (SOWFA) National Renewable Energy Laboratory, Golden, CO, USA 03 May 2012 <http://wind.nrel.gov/designcodes/simulators/sowfa/> accessed June 2013
- [20] Xfoil <http://web.mit.edu/drela/Public/web/xfoil/> accessed August 2012
- [21] Somers DM 2005 The S825 and S826 airfoils. National Renewable Energy Laboratory, NREL/SR-500-3634
- [22] Krogstad PÅ and Amund JA 2011 An experimental and numerical study of the performance of a model turbine. *Wind Energy* Wiley Online Library 13 June 2011 DOI: 10.1002/we.482
- [23] Fredriksen T 2013 Wind energy; CFD simulation of wakes and wind turbine forces. Master’s thesis spring 2013, Telemark University College, Faculty of Technology, Porsgrunn, Norway
- [24] Issa RI 1985 Solution of the implicitly discretized fluid flow equations by operator-splitting. *J. Comput. Phys.* **62** 40-65 ISSN 0021-9991
- [25] Martínez LA, Leonardi S, Churchfield MJ and Moriarty PJ 2012 A comparison of actuator disc and actuator line wind turbine models and best practices for their use. *50th AIAA Aerospace Sciences Meeting and Exhibit*, Nashville, TN, Jan. 9–12, AIAA, Washington D.C., 2012.
- [26] Churchfield MJ, Lee S, Michalakes J and Moriarty PJ A numerical study of the effects of atmospheric and wake turbulence on wind turbine dynamics. *J. Turbul.* Available online: 02 May 2012
- [27] Nodeland AM 2013 Wake modelling using an actuator disk model in openFOAM. Master’s thesis

- spring 2013, Norwegian University of Science and Technology, Department of Energy and Process Engineering, EPT-M-2013-85, Trondheim, Norway
- [28] Menter FR 1994 Two-equation eddy-viscosity turbulence models for engineering applications. *AIAA Journal*, **32**(8):1598-1605 August 1994